Contact Representations of Non-Planar Graphs

J. Alam[1], W. Evans[2], S. Kobourov[1], S. Pupyrev[1], J. Toeniskoetter[1], and T. Ueckerdt[3]

[1] Department of Computer Science, University of Arizona, USA
[2] Department of Computer Science, University of British Columbia, Canada
[3] Department of Mathematics, Karlsruhe Institute of Technology, Germany

Abstract. We study contact representations of non-planar graphs in which vertices are represented by axis-aligned polyhedra in 3D and edges are realized by non-zero area common boundaries between corresponding polyhedra. We present a liner-time algorithm constructing a representation of a 3-connected planar graph, its dual, and the vertex-face incidence graph with 3D boxes. We then investigate contact representations of 1-planar graphs. We first prove that optimal 1-planar graphs without separating 4-cycles admit a contact representation with 3D boxes. However, since not every optimal 1-planar graph can be represented in this way, we also consider contact representations with the next simplest axis-aligned 3D object, L-shaped polyhedra. We provide a quadratic-time algorithm for representing optimal 1-planar graphs with L-shapes.

1 Introduction

Graphs are often used to describe relationships between objects, and graph embedding techniques allow us to visualize such relationships. There are compelling theoretical and practical reasons to study *contact representations* of graphs, where vertices are geometric objects and edges correspond to pairs of objects touching in some specified fashion. In practice, 2D contact representations with rectangles, circles, and polygons of low complexity are intuitive, as they provide the viewer with the familiar metaphor of geographical maps. Such representations are preferred in some contexts over the standard node-link representations for displaying relational information [7].

A large body of work considers representing graphs by contacts of simple curves or polygons in 2D. Graphs that can be represented in this way are planar and Koebe's 1936 theorem established that *all* planar graphs can be represented by touching disks [16]. Every planar graph also has a contact representation with triangles [13]. Curves, line-segments, and L-shapes have also been used [12, 15]. In particular, it is known that all planar bipartite graphs can be represented by contacts of axis-aligned segments [8]. For non-planar graphs such contact representations in 2D are impossible. In a natural generalization for non-planar graphs, vertices can be represented with 3D-polyhedra. For example, representations of complete graphs and complete bipartite graphs using spheres and cylinders have been considered [4, 14]. Overall, there is very little known about such contact representations of non-planar graphs.

As a first step towards representing non-planar graphs, we consider *primal-dual* contact representations, in which a plane graph (a planar graph with a fixed planar embedding), its dual graph, and the face-vertex incidence graph are all represented simultaneously. More formally, in such a representation vertices and faces are represented by some geometric objects so that:

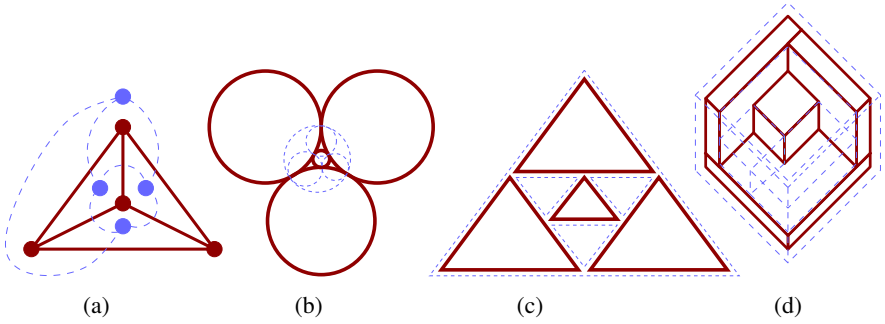

Fig. 1: (a) A plane graph K_4 and its dual; primal-dual contact representations of the graph with (b) circles and (c) triangles. (d) The primal-dual box-contact representation of K_4 with dual vertices shown dashed. The outer box (shell) contains all other boxes.

(i) the objects for the vertices are interior-disjoint and induce a contact representation for the primal graph;
(ii) the objects for the faces are interior-disjoint except for the object for the outer face, which contains all the objects for the internal faces, and together they induce a contact representation of the dual graph;
(iii) the objects for a vertex v and a face f of the primal graph intersect if and only if v and f are incident.

Primal-dual representations of plane graphs have been studied in 2D. Specifically, every 3-connected plane graph has a primal-dual representation with circles [1] and triangles [13]; see Fig. 1(a)–(c). Our first result in this paper is an analogous primal-dual representation using axis-aligned 3D boxes. While it is known that every planar graph has a contact representation with 3D boxes [5, 10, 21], Theorem 1 strengthens these results; see Fig. 1d.

Theorem 1. *Every 3-connected plane graph $G = (V, E)$ admits a proper primal-dual box-contact representation in 3D and it can be computed in $\mathcal{O}(|V|)$ time.*

Before proving this theorem we point out two important differences between our result for box-contact representation and the earlier primal-dual representations for circles and triangles [1, 13]. First, the existing constructions induce *non-proper* (point) contacts, while our contacts are always *proper*, that is, have non-zero areas. Second, for a given 3-connected plane graph, it is not always possible to find a primal-dual representation with circles by a polynomial-time algorithm, although it can be constructed numerically by polynomial-time iterative schemes [17]. There is also no known polynomial-time algorithm that computes a primal-dual representation with triangles for a given plane graph. In contrast, our box-contact representation can be computed in linear time and can be realized on the $\mathcal{O}(n) \times \mathcal{O}(n) \times \mathcal{O}(n)$ grid, where n is the number of vertices of the graph.

We prove Theorem 1 with a constructive algorithm, which uses the notions of Schnyder woods and orthogonal surfaces, as defined in [11]. It is known that every 3-connected planar graph induces an orthogonal surface; we will show how to construct a new contact representation with interior-disjoint boxes from such an orthogonal surface. Since the orthogonal surfaces for a 3-connected planar graph and its dual coincide

topologically, we show how to *geometrically* realize the primal and the dual box-contact representations so that they fit together to realize all the desired contacts. The construction idea is inspired by recent box-contact representation algorithms for maximal planar graphs [5]. Note, however, that we generalize one such algorithm to handle 3-connected planar graphs (rather than maximal-planar graphs) and show how to combine the primal and dual representations. Our method relies on a correspondence between Schnyder woods and generalized canonical orders for 3-connected planar graphs. Although the correspondence has been claimed in [2], the earlier proof appears to be incomplete. We provide a complete proof of the claim in Section B.2.

Theorem 1 immediately gives box-contact representations for a special class of non-planar graphs that are formed by the union of a planar graph, its dual, and the vertex-face incidence graph. The graphs were called *prime* by Ringel [18], who studied them in the context of simultaneously coloring a planar graph and its dual, and are defined as follows. A simple graph $G = (V, E)$ is said to be 1-*planar* if it can be drawn on the plane so that each of its edges crosses at most one other edge. A 1-planar graph has at most $4|V| - 8$ edges and it is *optimal* if it has exactly $4|V| - 8$ edges [9], that is, it is the densest 1-planar graph on the vertex set. An optimal 1-planar graph is called *prime* if it has no separating 4-cycles, that is, cycles of length 4 whose removal disconnects the graph. These optimal 1-planar graphs are exactly the ones that are 5-connected; alternatively, these graphs can be obtained as the union of a 3-connected simple plane graph, its dual and its vertex-face-incidence graph [19].

As in earlier primal-dual contact representations, it is not possible to have all vertex-objects interior disjoint. Specifically, one vertex-object (be it triangle, circle, or box) contains all the others. We call this special box the *shell* and such a representation a *shelled* box-contact representation. Here all the vertices are represented by 3D boxes, except for one vertex, which is represented by a shell, and the interiors of all the boxes and the exterior of the shell are disjoint. Note that a similar shell is also required in the circle-contact and triangle-contact representations; see Fig. 1. The following is a direct corollary of Theorem 1.

Corollary 1. *Every prime* 1*-planar graph* $G = (V, E)$ *admits a shelled box-contact representation in 3D and it can be computed in* $\mathcal{O}(|V|)$ *time.*

One may wonder whether every 1-planar graph admits a box-contact representation in 3D, but it is easy to see that there are 1-planar graphs, even as simple as K_5, that do not admit a box-contact representation. Furthermore, there exist optimal 1-planar graphs (which contain separating 4-cycles) that have neither a box-contact representation nor a shelled box-contact representation; for details see Lemma 5 in Appendix.

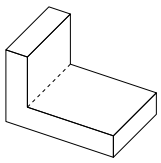

Fig. 2: An L-shaped polyhedron.

Therefore, we consider representations with the next simplest axis-aligned object in 3D, an L-shaped polyhedron or simply an $\mathcal{L}$, which is an axis-aligned box minus the intersection of two axis-aligned half-spaces; see Fig. 2. An $\mathcal{L}$ can also be considered the union of two 3D boxes. Note that the union of two axis-aligned boxes does not always form an $\mathcal{L}$ (e.g., it could form a T-shape); an $\mathcal{L}$ is the simplest of all such polyhedra. We provide a quadratic-time algorithm for representing every optimal 1-planar graph with $\mathcal{L}$'s.

Theorem 2. *Every embedded optimal* 1*-planar graph* $G = (V, E)$ *has a proper* $\mathcal{L}$*-contact representation in 3D and it can be computed in* $\mathcal{O}(|V|^2)$ *time.*

Our algorithm is similar to a recursive procedure used for constructing box-contact representations of planar graphs in [10,21]. The basic idea is to find separating 4-cycles and represent the inner and the outer parts of the graph induced by the cycles separately. Then these parts are combined to produce the final representation. Since the separating 4-cycles can be nested inside each other, the running time of our algorithm is dominated by the time required to find separating 4-cycles and their nested structure. Unlike the early algorithms for box-contact representations of planar graphs [10, 21], our algorithms produce proper contacts between the 3D objects (boxes and $\mathcal{L}$'s).

2 Primal-Dual Representations of 3-Connected Plane Graphs

Here we prove Theorem 1. Specifically, we describe a linear-time algorithm that computes a box-contact representation for the primal graph and the dual graph separately and then fits them together to also realize the face-vertex incidence graph. We first require some concepts about Schnyder woods and ordered path partitions.

Let G be a 3-connected plane graph with a specified pair of vertices $\{v_1, v_2\}$ and a third vertex $v_3 \notin \{v_1, v_2\}$, such that v_1, v_2, v_3 are all on the outer face in that counterclockwise order. Add the edge (v_1, v_2) to the outer face of G (if it does not already contain it) such that v_3 remains on the outerface and call the augmented graph G'. Let $\Pi = (V_1, V_2, \ldots, V_L)$ be a partition of the vertices of G such that each V_i induces a path in G; Π is an *ordered path partition* of G if the following conditions hold:

(1) V_1 contains the vertices on the counterclockwise path from v_1 to v_2 on the outer cycle; $V_L = \{v_3\}$;
(2) for $1 \leq k \leq L$, the subgraph G_k of G' induced by the vertices in $V_1 \cup \ldots \cup V_k$ is 2-connected and internally 3-connected (that is, removing two internal vertices of G_k does not disconnect it); hence the outer cycle C_k of G_k is a simple cycle containing the edge (v_1, v_2);
(3) for $2 \leq k \leq L$, each vertex on C_{k-1} has at most one neighbor in V_k.

The pair (v_1, v_2) forms the *base-pair* for Π and v_3 is the *head vertex* of Π. For an ordered path partition $\Pi = (V_1, V_2, \ldots, V_L)$ of G, a vertex v of G has *label* k if $v \in V_k$. The *predecessors* of v are the neighbors of v with equal or smaller labels; the *successors* of v are the neighbors of v with equal or larger labels; see Fig. 3a.

Again consider the three specified vertices v_1, v_2, v_3 in that counterclockwise order on the outer face of G. For $i \in \{1, 2, 3\}$, add a half-edge from v_i reaching into the outer face. A *Schnyder wood* is an orientation and a coloring of all the edges of G (including the added half-edges) with the colors $1, 2, 3$ satisfying the following conditions:

(1) every edge e is oriented in either one (*uni-directional*) or two opposite directions (*bi-directional*). The edges are colored so that if e is bi-directional, the two directions (half-edges) have distinct colors;
(2) the half-edge at v_i is directed outwards and colored i;
(3) each vertex v has out-degree exactly one in each color, and the counterclockwise order of edges incident to v is: outgoing in color 1, incoming in color 2, outgoing in color 3, incoming in color 1, outgoing in color 2, incoming in color 3;
(4) there is no interior face whose boundary is a directed cycle in one color.

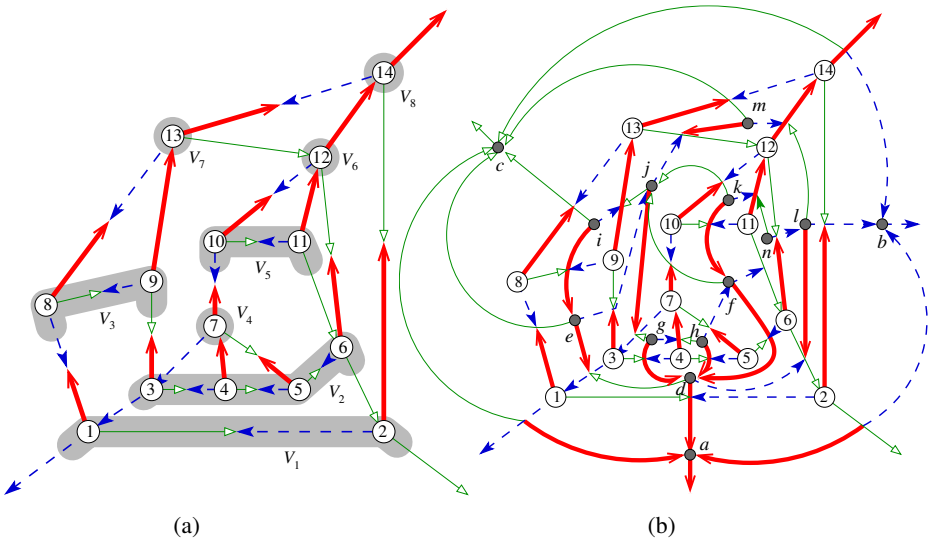

Fig. 3: (a) An ordered path partition and its corresponding Schnyder wood for a 3-connected graph G. (b) The Schnyder woods for the primal and the dual of G. The thick solid red, dotted blue and thin solid green edges represent the three trees in the Schnyder wood.

These conditions imply that for $i \in \{1, 2, 3\}$, the edges with color i induce a tree $\mathcal{T}_i$ rooted at v_i, where all edges of $\mathcal{T}_i$ are directed towards the root. Denote by $\mathcal{T}_i^{-1}$ the tree with all the edges of $\mathcal{T}_i$ reversed, and the Schnyder wood by $(\mathcal{T}_1, \mathcal{T}_2, \mathcal{T}_3)$. Every 3-connected plane graph has a Schnyder wood [3, 11]. From a Schnyder wood of a 3-connected plane graph G, one can construct a *dual Schnyder wood* (the Schnyder wood for the dual of G). Consider the dual graph G^* of G in which the vertex for the outer face of G has been split into three vertices forming a triangle. These three vertices represent the three regions between pairs of half edges from the outer vertices of G. Then a Schnyder wood for G^* is formed by orienting and coloring the edges so that between an edge e in G and its dual e^* in G^*, all three colors $1, 2, 3$ have been used. In particular, if e is uni-directional in color i, $i \in \{1, 2, 3\}$, then e^* is bi-directional in colors $i - 1$, $i + 1$ and vice versa; see Fig. 3b.

It is known that an ordered path partition of G defines a Schnyder wood on G, where the three outgoing edges for each vertex are to its (1) leftmost predecessor, (2) rightmost predecessor, and (3) highest-labeled successor [3, 11]. We call an ordered path partition and the corresponding Schnyder wood computed this way to be *compatible* with each other. Badent et al. [2] argue that the converse can also be done, that is, given a Schnyder wood on G, one can compute an ordered path partition, compatible with the Schnyder wood (and hence, there is a one-to-one correspondence between the concepts). However, the algorithm in [2] for converting a Schnyder wood to a compatible ordered path partition is incomplete, that is, the computed ordered path partition is not always compatible with the Schnyder wood. In Appendix B.2 we show such an example and provide a correction of the algorithm. Hence, we have:

Lemma 1. *Let $(\mathcal{T}_1, \mathcal{T}_2, \mathcal{T}_3)$ be a Schnyder wood of a 3-connected plane graph G with three specified vertices v_1, v_2, v_3 in that counterclockwise order on the outer face. Then for $i \in \{1, 2, 3\}$, one can compute in linear time an ordered path partition Π_i*

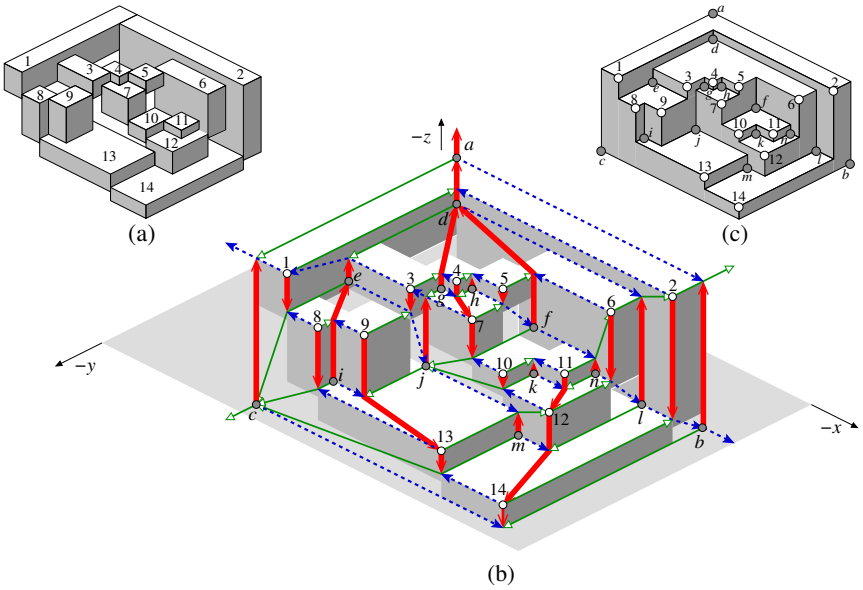

Fig. 4: Box-contact representation (a) for the graph in Fig. 3 with its primal-dual Schnyder wood (b) and the associated orthogonal surface (c). The thick solid red, dotted blue and thin solid green edges represent the three trees in the Schnyder wood.

compatible with $(\mathcal{T}_1, \mathcal{T}_2, \mathcal{T}_3)$ *such that* Π_i *has* (v_{i-1}, v_{i+1}) *as the base-pair and* v_i *as the head. The ordered path partition* Π_i *is consistent with the partial order defined by* $\mathcal{T}_{i-1}^{-1} \cup \mathcal{T}_{i+1}^{-1} \cup \mathcal{T}_i$.

We denote a connected region in a plane embedding of a graph by a *face*, and a side of a 3D shape by a *facet*. For a 3D box R, call the facet with highest (lowest) x-coordinate as the x^+-facet (x^--facet) of R. The y^+-facet, y^--facet, z^+-facet and z^--facets of R are defined similarly. For convenience, we sometimes denote the x^+-, x^--, y^+-, y^--, z^+- and z^--facets of R as the *right*, *left*, *front*, *back*, *top* and *bottom* facets of R, respectively. We are now ready to prove Theorem 1. We sketch the main idea; see Appendix B for a complete version.

Theorem 1. *Every 3-connected plane graph* $G = (V, E)$ *admits a proper primal-dual box-contact representation in 3D and it can be computed in* $\mathcal{O}(|V|)$ *time.*

Proof sketch. Our algorithm consists of the following steps. Let v_1, v_2 and v_3 be three vertices on the outer face of G in the counterclockwise order. First, we create a Schnyder wood $(\mathcal{T}_1, \mathcal{T}_2, \mathcal{T}_3)$ such that for $i \in \{1, 2, 3\}$, $\mathcal{T}_i$ is rooted at v_i. Then using Lemma 1, we compute three ordered path partitions compatible with $(\mathcal{T}_1, \mathcal{T}_2, \mathcal{T}_3)$. Next the ordered path partitions are used to calculate the coordinates of 3D boxes that form a contact representation for the primal graph G; a number of local modifications is performed to obtain proper contacts. Finally, the same steps are applied, starting with the dual Schnyder wood of $(\mathcal{T}_1, \mathcal{T}_2, \mathcal{T}_3)$, to construct the representation of the dual graph G^*. These two representations induce the same orthogonal surfaces [11]; hence, they can be combined together to form a primal-dual box-contact representation.

Note that a similar idea is used in [5] to compute a box-contact representation for a maximal planar graph. We strengthen the result by (1) generalizing the method to 3-connected planar graphs and (2) computing an ordered path partition compatible with a Schnyder wood. The latter guarantees the fit between the primal and the dual.

Let us sketch the steps for computing the primal representation from a Schnyder wood $(\mathcal{T}_1, \mathcal{T}_2, \mathcal{T}_3)$; the computation for the dual representation is analogous. By Lemma 1, for $i \in \{1, 2, 3\}$, one can compute a compatible ordered path partition with the base-pair (v_{i-1}, v_{i+1}) and head v_i, which is consistent with the partial order defined by $\mathcal{T}_{i-1}^{-1} \cup \mathcal{T}_{i+1}^{-1} \cup \mathcal{T}_i$. Denote by $<_X$, $<_Y$ and $<_Z$ the three ordered path partitions compatible with $(\mathcal{T}_1, \mathcal{T}_2, \mathcal{T}_3)$, that are consistent with $\mathcal{T}_3^{-1} \cup \mathcal{T}_2^{-1} \cup \mathcal{T}_1$, $\mathcal{T}_1^{-1} \cup \mathcal{T}_3^{-1} \cup \mathcal{T}_2$, and $\mathcal{T}_2^{-1} \cup \mathcal{T}_1^{-1} \cup \mathcal{T}_3$, respectively. For a vertex u, let $x_M(u)$, $y_M(u)$, and $z_M(u)$ be the labels of u in the ordered path partitions $<_X$, $<_Y$, and $<_Z$, respectively. Define $x_m(u) = x_M(b)$, $y_m(u) = y_M(g)$ and $z_m(u) = z_M(r)$, where b, g and r are the parents of u in $\mathcal{T}_1$, $\mathcal{T}_2$ and $\mathcal{T}_3$, respectively, whenever these parents are defined. For each of the three special vertices v_i, $i \in \{1, 2, 3\}$, the parent is not defined in $\mathcal{T}_i$. We assign $x_m(v_1) = 0$, $y_m(v_2) = 0$ and $z_m(v_3) = 0$. For each vertex u of G, define a box $R(u)$ as the region $[x_M(u), x_m(u)] \times [y_M(u), y_m(u)] \times [z_M(u), z_m(u)]$.

Lemma 7 in Appendix shows that the boxes defined above yield a box-contact representation for G. Similarly, a representation for the dual graph G^* is computed. These representations can be combined together; see Appendix B for more details. Finally, the three boxes for the three outer vertices of G^* are replaced by a single shell-box, which forms the boundary of the entire representation.

The algorithm runs in $\mathcal{O}(|V|)$ time since computing the primal and the dual Schnyder woods [11], computing ordered path partitions from Schnyder woods (Lemma 1), and the computation of the coordinates all can be accomplished in linear time. □

3 L-Contact Representation of Optimal 1-Planar Graphs

Here we prove Corollary 1 and Theorem 2. Throughout, let G be an optimal 1-planar graph with a fixed 1-planar embedding. An edge is *crossing* if it crosses another edge, and *non-crossing* otherwise. A cycle in a connected graph is *separating* if removing it disconnects the graph. We start by listing some well-known properties of optimal 1-planar graphs.

Lemma 2 (Brinkmann et al. [6], Suzuki [20]).

- *The subgraph of an embedded optimal 1-planar graph G induced by the non-crossing edges is a plane quadrangulation Q with bipartition classes W and B.*
- *The induced subgraphs $G_W = G[W]$ and $G_B = G[B]$ on white and black vertices, respectively, are planar and dual to each other.*
- *G_B and G_W are 3-connected if and only if Q has no separating 4-cycles.*
- *There exists a simple optimal 1-planar graph with quadrangulation Q if and only if Q is 3-connected.*

An optimal 1-planar graph is *prime* if its quadrangulation has no separating 4-cycle.

Corollary 1. *Every embedded prime 1-planar graph $G = (V, E)$ admits a shelled box-contact representation in 3D and it can be computed in $\mathcal{O}(|V|)$ time.*

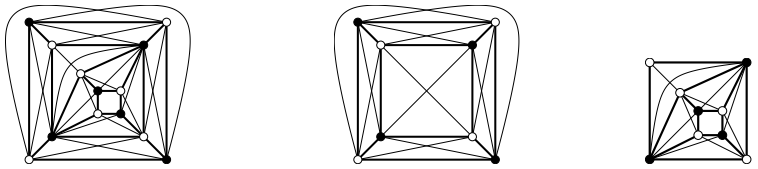

(a) (b) (c)

Fig. 5: (a) An embedded optimal 1-planar graph, its quadrangulation Q (bold) and the partition into white and black vertices. (b) The graph G_{out} produced by removing the interior of separating 4-cycle C. (c) The graph $G_{in}(C)$ comprised of the separating 4-cycle and its interior.

Proof. Let Q be the quadrangulation of G and let B, W be the bipartition classes of Q. By Lemma 2, $G_B = G[B]$ and $G_W = G[W]$ are 3-connected planar and dual to each other. By Theorem 1, a primal-dual box-contact representation Γ of G_B can be computed in linear time. We claim that Γ is a contact representation of G. Indeed, the edges of G are partitioned into G_B, G_W, Q. Each edge in G_B is realized by contact of two "primal" boxes, in G_W by contact of "dual" boxes, and in Q by contact of a primal and a dual box; see Fig. 15. □

Next, assume that G is any (not necessarily prime) optimal 1-planar graph. To find an $\mathcal{L}$-representation for G, we find all separating 4-cycles in G, replace their interiors by a pair of crossing edges and construct an $\mathcal{L}$-representation of the obtained smaller 1-planar graph by Corollary 1. We ensure that this $\mathcal{L}$-representation has some "available space" in which we can place the $\mathcal{L}$-representations for the removed subgraph in each separating 4-cycle, which we construct recursively. We remark that similar procedures were used before, e.g., for maximal planar graphs and their separating triangles [10,21]. A separating 4-cycle is *maximal* if its interior is inclusion-wise maximal among all separating 4-cycles. A 1-planar graph with at least 5 vertices is called *almost-optimal* if its non-crossing edges induce a quadrangulation Q and inside each face of Q, other than the outer face, there is a pair of crossing edges.

Algorithm *L-Contact*(optimal 1-planar graph G)

1. Find all separating 4-cycles in the quadrangulation Q of G
2. **if** some inner vertex w of Q is adjacent to two outer vertices of Q
3. **then** $\mathcal{C}$ = the two 4-cycles containing w and 3 outer vertices of Q. **(Case 1)**
   else $\mathcal{C}$ = set of all maximal separating 4-cycles in Q. **(Case 2)**
4. Take the optimal 1-planar (multi)graph G_{out} obtained from G by replacing for each 4-cycle $C \in \mathcal{C}$ all vertices strictly inside C by a pair of crossing edges; see Fig. 5b.
5. Compute an $\mathcal{L}$-representation of G_{out} with "some space" at each 4-cycle $C \in \mathcal{C}$. In Case 2, this is done by a shelled box-contact representation of G_{out} in Corollary 1.
6. For each $C \in \mathcal{C}$, take the almost-optimal 1-planar subgraph $G_{in}(C)$ of G induced by C and all vertices inside C; see Fig. 5c. Recursively compute an $\mathcal{L}$-representation of $G_{in}(C)$ and insert it into the corresponding "space" in the $\mathcal{L}$-representation of G_{out}.

Let us formalize the idea of "available space" mentioned in steps 5 and 6 in the above procedure. Let Γ be any $\mathcal{L}$-representation of some graph G and C be a 4-cycle in G. A *frame for* C is a 3-dimensional axis-aligned box F together with an injective

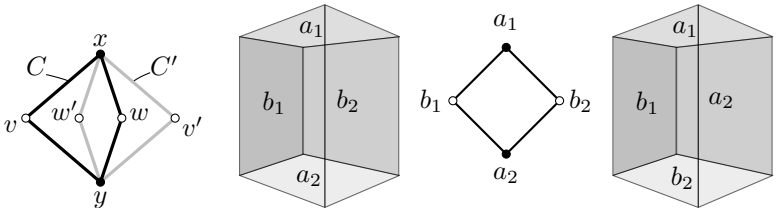

(a) (b)

Fig. 6: (a) Illustration for the proof of Lemma 3. (b) A frame of type $(\perp\!-\!||)$ (left) and of type $(\perp\!-\!\perp)$ (right).

mapping of $V(C)$ onto the facets of F such that the two facets without a preimage are adjacent. Every frame has one of two possible types. If two opposite vertices of C are mapped onto two opposite facets of F, then F has type $(\perp\!-\!||)$; otherwise, F has type $(\perp\!-\!\perp)$; see Fig. 6b. Finally, for an almost-optimal 1-planar graph G with corresponding quadrangulation Q and outer face C, and a given frame F for C, we say that an $\mathcal{L}$-representation Γ of G *fits into* F if replacing the boxes or $\mathcal{L}$'s for the vertices in C by the corresponding facets of F yields a proper contact representation of $G - E(G[C])$ that is strictly contained in F.

Before we prove Theorem 2, we need one last lemma addressing the structure of maximal separating 4-cycles in almost-optimal 1-planar graphs.

Lemma 3. *Let G be an almost-optimal 1-planar graph with corresponding quadrangulation Q. Then all maximal separating 4-cycles of Q are interior-disjoint, unless two inner vertices w and w' of Q are adjacent to two outer vertices of Q.*

Proof. When two maximal separating 4-cycles C and C' are not interior-disjoint, then some vertex from C lies strictly inside C' and some vertex from C' lies strictly inside C. It follows that $V(C) \cap V(C')$ is a pair x, y of two vertices from the same bipartition class of Q, say $x, y \in B$, and that some $v \in V(C)$ lies strictly outside C' and some $v' \in V(C')$ lies strictly outside C. We have $v, v' \in W$ and that $C^* = (x, v, y, v')$ is a 4-cycle whose interior strictly contains C and C'. By the maximality of C and C', C^* is not separating. Since the vertices $w \in V(C) \setminus V(C^*)$ and $w' \in V(C') \setminus V(C^*)$ lie strictly inside C^*, C^* is the outer cycle of Q and w, w' are the desired vertices. □

Theorem 2. *Every embedded optimal 1-planar graph $G = (V, E)$ has a proper $\mathcal{L}$-contact representation in 3D and it can be computed in $\mathcal{O}(|V|^2)$ time.*

Proof. Let Q be the quadrangulation of G with outer cycle C_{out}. Following algorithm **L-Contact**, we distinguish two cases. If (**Case 1**) some inner vertex w of Q has two neighbors on C_{out} we let $\mathcal{C}$ be the set of the two 4-cycles in Q that consist of w and 3 vertices of C_{out}. Otherwise (**Case 2**), let $\mathcal{C}$ be the set of all maximal separating 4-cycles in Q. By Lemma 3 the cycles in $\mathcal{C}$ are interior-disjoint. As in step 4 we define G_{out} to be the optimal 1-planar (multi)graph obtained from G by replacing for each $C \in \mathcal{C}$ all vertices strictly inside C by a pair of crossing edges. Note that in Case 1 the quadrangulation corresponding to G_{out} is $K_{2,3}$ with inner vertex w. We proceed by proving the following lemma, which corresponds to step 5 in the algorithm.

Lemma 4. *Let H be an almost-optimal 1-planar (multi)graph whose corresponding quadrangulation Q_H is either $K_{2,3}$ or has no separating 4-cycles. Let $\mathcal{C}$ be a set of facial 4-cycles of Q_H, different from C_o, and H' be the graph obtained from H by removing the crossing edges in each $C \in \mathcal{C}$. Then for any given frame F for the outer cycle C_o of Q_H one can compute an $\mathcal{L}$-representation Γ of H' fitting into F so that for every $C \in \mathcal{C}$ there is a frame $F_C \subseteq F$ that is interior-disjoint from all boxes and $\mathcal{L}$'s.*

Proof. **Case 1, $Q_H = K_{2,3}$.** Let w be the inner vertex of H. Without loss of generality let $F = [0,5]\times[0,5]\times[0,4]$ and let $V(C_o)$ be mapped onto the top, back left, bottom and back right facets of F. Define the $\mathcal{L}$ for w to be the union of $[0,3]\times[2,3]\times[0,4]$ and $[2,3]\times[0,3]\times[0,4]$. Define four boxes $F_1 = [0,2]\times[0,1]\times[0,1]$, $F_2 = [0,2]\times[0,1]\times[3,4]$, $F_3 = [3,4]\times[0,1]\times[0,4]$ and $F_4 = [0,1]\times[3,4]\times[0,4]$, each completely contained in F and disjoint from the $\mathcal{L}$ for w; see Fig. 7. Each F_i, $ii \in \{1,2,3,4\}$ is a frame for a 4-tuple containing w and three vertices of C_o. Thus independent of the type of F and the neighbors of w in Q_H, we find a frame for the inner faces of Q_H.

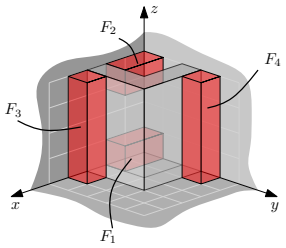

Fig. 7: Construction for Case 1 in the proof of Lemma 4.

Case 2, $Q_H \neq K_{2,3}$. Let B and W be the bipartition classes of Q_H and $C_o = (v_1, w_1, v_2, w_2)$ with $v_i \in B$ and $w_i \in W$, $i = 1, 2$. Without loss of generality v_1, v_2, w_1 are mapped onto the back left, back right and top facets of F, respectively, and w_2 is mapped onto the bottom facet if (**Case 2.1**) F has type $(\perp-||)$ and onto the front left facet if (**Case 2.2**) F has type $(\perp-\perp)$. Let H^* be the graph obtained from H by inserting a pair of crossing edges in C_o, leaving v_1, w_2 and v_2 on the unbounded region. By assumption, H^* is a prime 1-planar graph and thus by Lemma 2 $H^*_B = H^*[B]$ and $H^*_W = H^*[W]$ are planar 3-connected and dual to each other. We choose v_3 to be the clockwise next vertex after v_2 on the outer face of H^*_B and compute (using Corollary 1) a shelled box-contact representation Γ^* of H^*, in which w_2 is represented as the bounding box $F^* = [0,n]^3$, $n \in \mathbb{N}$, and v_1, v_2, w_1 as $[0,n]\times[0,1]\times[0,n]$, $[0,1]\times[0,n]\times[1,n]$ $\times[1,n]\times[n-1,n]$, i.e., these boxes constitute the back left, back right and top facets of F^*, respectively.

Next we show how to create a frame for each facial 4-cycle $C \in \mathcal{C}$. Let a_1, b_1, a_2, b_2 be the vertices of C in cyclic order. Assume without loss of generality that $a_1, a_2 \in W$ and $b_1, b_2 \in B$. Thus (a_1, a_2) and (b_1, b_2) are crossing edges of H^*_W and H^*_B, respec-

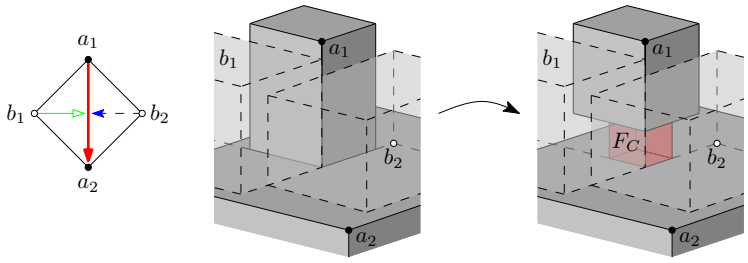

Fig. 8: Creating a frame F_C for an inner facial cycle $C = (a_1, b_1, a_2, b_2)$ of Q_H by releasing the contact between a_1 and a_2.

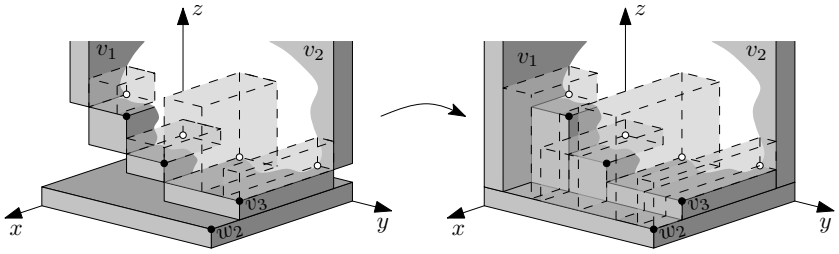

Fig. 9: Modifying Γ' when F has type $(\perp - ||)$ (Case 2.1) to find a representation fitting F.

tively. In the Schnyder wood of H_W^* underlying Corollary 1 exactly one of (a_1, a_2), (b_1, b_2) is uni-directed, say (a_1, a_2) is uni-directed in tree $\mathcal{T}_1$. Then there is a point in $\mathbb{R}^3$ in common with all four boxes in Γ^* corresponding to vertices of C. Moreover, by Lemma 7 boxes b_1, a_2, b_2 touch box a_1 with their y^+, z^+, y^- facets, respectively; see Fig. 8. Now we can increase the lower z-coordinate of the box a_1 by some $\varepsilon > 0$ so that a_1 and a_2 lose contact and between these two boxes a cubic frame F_C with side length ε is created; see again Fig. 8. Note that by Lemma 7 the z^- facet of a_1 makes contact only with a_2 and hence if ε is small enough all other contacts in Γ^* are maintained. We apply this operation to each $C \in \mathcal{C}$ and obtain a shelled box-representation Γ' of H'.

Finally, we show how to modify Γ' to obtain an $\mathcal{L}$-representation of H' fitting the given frame F. If (**Case 2.1**) F has type $(\perp - ||)$, we define a new box for w_2 to be $[0, n+1] \times [0, n] \times [-1, 0]$. For each white neighbor of w_2 we union the corresponding box with another box that is contained in $[n, n+1] \times [0, n] \times [0, n]$ with bottom facet at $z = 0$ so that the result is an $\mathcal{L}$-shape. For each black neighbor of w_2 we set the lower z-coordinate of the corresponding box to 0; see Fig. 9. (This requires the proper contacts for outer edges of G_B, except for (v_1, v_2), to be parallel to the xz-plane, which we can easily guarantee.) We then apply an affine transformation mapping $[1, n+1] \times [1, n] \times [0, n-1]$ onto F. If (**Case 2.2**) F has type $(\perp - \perp)$, define a new box for w_2 to be $[0, n] \times [n, n+1] \times [0, n]$ and apply an affine transformation mapping $[1, n] \times [1, n] \times [0, n-1]$ to F. In both cases we have an $\mathcal{L}$-representation of H' fitting F. □

By the lemma above we can compute an $\mathcal{L}$-representation Γ_{out} of G_{out} fitting any given frame F_{out} for C_{out} in $\mathcal{O}(|V(G_{out})|)$ time. Moreover, Γ_{out} has a set of disjoint frames $\{F_C \mid C \in \mathcal{C}\}$. Following step 6 of algorithm **L-Contact**, for each $C \in \mathcal{C}$, let $G_{in}(C)$ be the almost-optimal 1-planar graph given by all vertices and edges of G on and strictly inside C. Recursively applying the lemma we can compute an $\mathcal{L}$-representation Γ_C of $G_{in}(C)$ fitting the frame F_C for C in Γ_{out}. Clearly, $\Gamma = \Gamma_{out} \cup \bigcup_{C \in \mathcal{C}} \Gamma_C$ is an $\mathcal{L}$-representation of G fitting F_{out}. We pick a frame F_{out} of arbitrary type for C_{out} to complete the construction. Although computing an $\mathcal{L}$-representation of G_{out} takes $\mathcal{O}(|V(G_{out})|)$ time, recursive computation and affine transformations on the $\mathcal{L}$'s for the vertices in $G_{in}(C)$ for each $C \in \mathcal{C}$ require $\mathcal{O}(|V|^2)$ time. □

4 Conclusion and Open Questions

We described efficient algorithms for 3D contact representation of several types on non-planar graphs. Many interesting problems remain open. A planar graph has a contact representation with rectangles in 2D if and only if it has no separating triangles. Is

there a similar characterization for 3D box-contact representations? It is known that any planar graph admits a proper contact representation with boxes in 3D and a non-proper contact representation with cubes (boxes with equal sides). Does every planar graph admit a proper contact representation with cubes? Representing graphs with contacts of constant-complexity 3D shapes, such as $\mathcal{L}$'s, is open for many graph classes with a linear number of edges, such as 1-planar, quasi-planar and other nearly planar graphs.

References

1. Andreev, E.: On convex polyhedra in Lobachevskii spaces. Mat. Sb. 123(3), 445–478 (1970)
2. Badent, M., Brandes, U., Cornelsen, S.: More canonical ordering. Journal of Graph Algorithms and Applications 15(1), 97–126 (2011)
3. Bernardi, O., Fusy, E.: Schnyder decompositions for regular plane graphs and application to drawing. Algorithmica 62(3–4), 1159–1197 (2012)
4. Bezdek, A.: On the number of mutually touching cylinders. Combinatorial and Computational Geometry 52, 121–127 (2005)
5. Bremner, D., Evans, W., Frati, F., Heyer, L., Kobourov, S., Lenhart, W., Liotta, G., Rappaport, D., Whitesides, S.: Representing graphs by touching cuboids. In: Graph Drawing. LNCS, vol. 7704, pp. 187–198. Springer (2013)
6. Brinkmann, G., Greenberg, S., Greenhill, C., McKay, B., Thomas, R., Wollan, P.: Generation of simple quadrangulations of the sphere. Discrete Math. 305(1–3), 33–54 (2005)
7. Buchsbaum, A.L., Gansner, E.R., Procopiuc, C.M., Venkatasubramanian, S.: Rectangular layouts and contact graphs. ACM Transactions on Algorithms 4(1) (2008)
8. Czyzowicz, J., Kranakis, E., Urrutia, J.: A simple proof of the representation of bipartite planar graphs as the contact graphs of orthogonal straight line segments. Information Processing Letters 66(3), 125–126 (1998)
9. Fabrici, I., Madaras, T.: The structure of 1-planar graphs. Discrete Mathematics 307(7–8), 854–865 (2007)
10. Felsner, S., Francis, M.C.: Contact representations of planar graphs with cubes. In: Hurtado, F., van Kreveld, M.J. (eds.) SOCG. pp. 315–320. ACM (2011)
11. Felsner, S., Zickfeld, F.: Schnyder woods and orthogonal surfaces. Discrete & Computational Geometry 40(1), 103–126 (2008)
12. de Fraysseix, H., de Mendez, P.O.: Representations by contact and intersection of segments. Algorithmica 47(4), 453–463 (2007)
13. Gonçalves, D., Lévêque, B., Pinlou, A.: Triangle contact representations and duality. Discrete & Computational Geometry 48(1), 239–254 (2012)
14. Hliněný, P., Kratochvíl, J.: Representing graphs by disks and balls (a survey of recognition-complexity results). Discrete Mathematics 229(1–3), 101–124 (2001)
15. Kobourov, S.G., Ueckerdt, T., Verbeek, K.: Combinatorial and geometric properties of planar Laman graphs. In: Khanna, S. (ed.) SODA. pp. 1668–1678. SIAM (2013)
16. Koebe, P.: Kontaktprobleme der konformen Abbildung. Berichte über die Verhandlungen der Sächsischen Akad. der Wissen. zu Leipzig. Math.-Phys. Klasse 88, 141–164 (1936)
17. Mohar, B.: Circle packings of maps in polynomial time. European Journal of Combinatorics 18(7), 785–805 (1997)
18. Ringel, G.: Ein sechsfarbenproblem auf der kugel. Abhandlungen aus dem Mathematischen Seminar der Universitat Hamburg 29(1–2), 107–117 (1965)
19. Schumacher, H.: Zur struktur 1-planarer graphen. Math. Nachrichten 125, 291–300 (1986)
20. Suzuki, Y.: Re-embeddings of maximum 1-planar graphs. SIAM Journal on Discrete Mathematics 24(4), 1527–1540 (2010)
21. Thomassen, C.: Interval representations of planar graphs. Journal of Combinatorial Theory Series B 40(1), 9–20 (1988)

Appendix

Acknowledgments

We thank Michael Bekos, Therese Biedl, Franz Brandenburg, Michael Kaufmann, Giuseppe Liotta for useful discussions about different variants of these problems. We also thank the anonymous reviewers of an earlier version of the paper for constructive criticism and suggestions for improvement.

A 1-Planar Graphs with no Box-Contact Representation

Lemma 5.

- K_5 *has no proper box-contact representation in 3D.*
- *There exist optimal* 1*-planar graphs that have neither box-contact representation nor shelled box-contact representation in 3D.*

Proof. Assume for a contradiction that K_5 has a contact representation Γ with five boxes B_i, $i \in \{1, 2, 3, 4, 5\}$. We first show that there is a point o, which is common to all five boxes in Γ, that is, $\cap_{i=1}^{5} B_i$ is not empty. Since B_i is an axis-aligned box, one can define B_i as $[x_i, X_i] \times [y_i, Y_i] \times [z_i, Z_i]$ for each $i \in \{1, 2, 3, 4, 5\}$. Now for any pair of boxes B_i and B_j, $i, j \in \{1, 2, 3, 4, 5\}$, B_i and B_j make a contact in Γ since it represents K_5; hence there is a point (x_{ij}, y_{ij}, z_{ij}) common to B_i and B_j. This can happen only if $x_{ij} \in [x_i, X_i]$, $x_{ij} \in [x_j, X_j]$, $y_{ij} \in [y_i, Y_i]$, $y_{ij} \in [y_j, Y_j]$ and $z_{ij} \in [z_i, Z_i]$, $z_{ij} \in [z_j, Z_j]$. In particular if we look at the projection on the x-axis, $x_i \leq x_{ij} \leq X_i$ and $x_j \leq x_{ij} \leq X_j$; that is, $[x_i, X_i]$ and $[x_j, X_j]$ have a common point x_{ij}. Then by Helly's theorem [22], all $[x_i, X_i]$, $i \in \{1, 2, 3, 4, 5\}$ have a common point x^*. Similarly, all the projections of B_i's on the y-axis (resp. on the z-axis) have a common point y^* (resp. z^*). Then for each box B_i, $(x^*, y^*, z^*) \in B_i$. Therefore (x^*, y^*, z^*) is a common point for all five boxes. Call this point o.

Now consider the eight closed octants with o in the center. Denote the positive and negative x-half-space of o by x_+ and x_-, respectively. Similarly define y_+, y_-, z_+ and z_- to be the positive y-half-space, negative y-half-space, positive z-half-space and negative z-half-space, respectively. Then for $X \in \{x_+, x_-\}$, $Y \in \{y_+, y_-\}$, $Z \in \{z_+, z_-\}$, denote the octant $X \cap Y \cap Z$ by XYZ. Since all five boxes contain o, no octant can contain parts of two or more boxes. Since there are eight octants and five boxes,

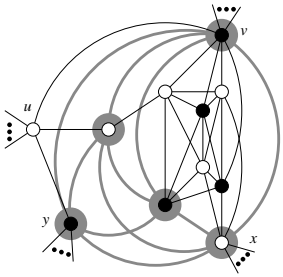

Fig. 10: An almost optimal 1-planar graph G^* containing a K_5 (highlighted).

by pigeonhole principle, there are at least two boxes, each of which are completely contained inside one octant. Assume, w.l.o.g. (after possible renaming), that B_1 and B_2 are these two boxes and they lie on the two octants $x_+y_+z_+$ and $x_+y_+z_-$, respectively. Then for any box to make a proper contact with both B_1 and B_2, it must lie either in both the octants $x_-y_+z_+$, $x_-y_+z_-$, or in both the octants $x_+y_-z_+$, $x_+y_-z_-$. This implies that at least one of the three boxes B_3, B_4 and B_5 fails to make a proper contact with at least one of B_1 and B_2. This completes the proof for the first part of the lemma.

In order to prove the second part of the claim, note that there exists an almost-optimal 1-planar graph containing K_5 as a subgraph; see Fig. 10. Call this graph G^*. Now consider an optimal 1-planar graph G. Take two faces $f_1 = a_1b_1c_1d_1$ and $f_2 = a_2b_2c_2d_2$ in the quadrangulation of G such that they do not share vertices. Delete the crossing edges inside the two faces and in each face f_i, $i = 1, 2$, and insert an isomorphic copy of G^*, identifying u, v, x, y with a_i, b_i, c_i, d_i. Let H be the resulting augmented graph. As shown earlier, H has no contact representation with interior-disjoint boxes. Furthermore, H does not admit a shelled box-contact representation, as at least one copy of G^* in H does not contain the vertex represented by the shell. □

B Proof of Theorem 1

First we introduce the tools needed to prove Theorem 1. We define the known concepts of an *ordered path partition* and a *Schnyder wood*. Then we describe new results about the relationship between these two structures for 3-connected plane graphs. Then we review the concept of an *orthogonal surface*.

B.1 Ordered Path Partitions and Schnyder Woods

The concepts of a Schnyder wood and a canonical order were initially introduced for maximal plane graphs [25, 28]; later they were generalized to 3-connected plane graphs [23, 27]. Although the concepts are proved to be equivalent for maximal plane graphs [24], they are no longer equivalent after the generalization. Thus Badent et al. [2] generalized the notion of a canonical order to an *ordered path partition* for a 3-connected plane graph in an attempt to make it equivalent to a Schnyder wood.

Let G be a 3-connected plane graph with a specified pair of vertices $\{v_1, v_2\}$ and a third vertex $v_3 \notin \{v_1, v_2\}$, such that v_1, v_2, v_3 are all on the outer face in that counterclockwise order. Add the edge (v_1, v_2) to the outer face of G (if it does not already contain it) such that v_3 remains on the outerface and call the augmented graph G'. Let $\Pi = (V_1, V_2, \ldots, V_L)$ be a partition of the vertices of G such that each V_i induces a path P_i in G; Π is an *ordered path partition* of G if the following conditions hold:

(1) V_1 contains the vertices on the counterclockwise path from v_1 to v_2 on the outer cycle; $V_L = \{v_3\}$;
(2) for $1 \leq k \leq L$, the subgraph G_k of G' induced by the vertices in $V_1 \cup \ldots \cup V_k$ is 2-connected and internally 3-connected (that is, removing two internal vertices of G_k does not disconnect it); hence the outer cycle C_k of G_k is a simple cycle containing the edge (v_1, v_2);
(3) for $2 \leq k \leq L$, each vertex on C_{k-1} has at most one neighbor on P_k.

Note that the above definition is a slight generalization of the definition in [2], in that P_1 does not necessarily consists of a single edge, but is otherwise equivalent. The

pair of vertices (v_1, v_2) forms the *base-pair* for Π and v_3 is called the *head vertex* of Π. For an ordered path partition $\Pi = (V_1, V_2, \ldots, V_L)$ of G, we say that a vertex v of G has *label* k if $v \in V_k$. The *predecessors* of v are all the neighbors of v with equal or smaller labels; and the *successors* of v are all neighbors of v with equal or larger labels; see Fig. 3a.

A Schnyder wood is defined as follows. Let v_1, v_2, v_3 be three specified vertices in that counterclockwise order on the outer face of G. For $i \in \{1, 2, 3\}$, add a half-edge from v_i reaching into the outer face. Then a *Schnyder wood* is an orientation and coloring of all the edges of G (including the added half edges) with the colors $1, 2, 3$ satisfying the following conditions:

(1) every edge e is oriented in either one (*uni-directional*) or two opposite directions (*bi-directional*). The directions of edges are colored such that if e is bi-directional, then the two directions have distinct colors;
(2) the half-edge at v_i is directed outwards and colored i;
(3) each vertex v has out-degree exactly one in each color, and the counterclockwise order of edges incident to v is: outgoing in color 1, incoming in color 2, outgoing in color 3, incoming in color 1, outgoing in color 2, incoming in color 3;
(4) there is no interior face whose boundary is a directed cycle in one color.

These conditions imply that for $i \in \{1, 2, 3\}$, the edges with color i induce a tree $\mathcal{T}_i$ rooted at v_i, where all edges of $\mathcal{T}_i$ are directed towards the root. We denote the Schnyder wood by $(\mathcal{T}_1, \mathcal{T}_2, \mathcal{T}_3)$. Every 3-connected plane graph has a Schnyder wood [3,11]. From a Schnyder wood of a 3-connected plane graph G, one can construct a *dual Schnyder wood* (the Schnyder wood for the dual of G). Consider the dual graph G^* of G in which the vertex for the outer face of G has been split into three vertices forming a triangle. These three vertices represent the three regions between pairs of half edges from the outer vertices of G. Then a Schnyder wood for G^* is formed by orienting and coloring the edges so that between an edge e in G and its dual e^* in G^*, all three colors $1, 2, 3$ have been used. In particular, if e is uni-directional in color i, $i \in \{1, 2, 3\}$, then e^* is bi-directional in colors $i - 1$, $i + 1$ and vice versa; see Fig. 3b.

B.2 Correspondence

Let G be a 3-connected plane graph with a specified base-pair (v_1, v_2) and a specified head vertex v_3 such that v_1, v_2, v_3 are in that counterclockwise order on the outer face. It is known that an ordered path partition of G defines a Schnyder wood on G, where the three outgoing edges for each vertex are to its (1) leftmost predecessor, (2) rightmost predecessor, and (3) highest-labeled successor [3, 11]. We call an ordered path partition and the corresponding Schnyder wood computed this way to be *compatible* with each other. Badent et al. [2] claim that the converse can also be done, that is, given a Schnyder wood on G, one can compute an ordered path partition, compatible with the Schnyder wood (and hence, there is a one-to-one correspondence between the concepts). However, it turns out that the algorithm in [2] for converting a Schnyder wood to a compatible ordered path partition is incomplete[4], that is, the computed ordered path partition is not always compatible with the Schnyder wood; see Fig. 11 for an example. Here we provide a correction for the algorithm.

[4] Confirmed by a personal communication with the authors of [2].

Let $(\mathcal{T}_1, \mathcal{T}_2, \mathcal{T}_3)$ be a Schnyder wood of G. From here on whenever we talk about Schnyder woods, we consider a circular order for the indices $i \in \{1, 2, 3\}$ so that $(i-1)$ and $(i+1)$ are well defined when $i \in \{1, 2, 3\}$. Denote by $\mathcal{T}_i^{-1}$ the tree with all the edges of $\mathcal{T}_i$ reversed. The following Lemma is due to [2, 11] and gives an important property for $\mathcal{T}_{i-1}^{-1} \cup \mathcal{T}_{i+1}^{-1} \cup \mathcal{T}_i$, which is the graph on the vertices of G obtained by taking the edge directions of $\mathcal{T}_{i-1}^{-1}$, $\mathcal{T}_{i+1}^{-1}$ and $\mathcal{T}_i$.

Lemma 6 (Badent et al. [2], Felsner and Zickfeld [11]).

Let $(\mathcal{T}_1, \mathcal{T}_2, \mathcal{T}_3)$ be a Schnyder wood of a 3-connected plane graph G. Then $\mathcal{T}_{i-1}^{-1} \cup \mathcal{T}_{i+1}^{-1} \cup \mathcal{T}_i$ does not contain any directed simple cycle of length greater than two. The directed simple cycles of length two are induced by the bi-directional edges with colors $i-1$, $i+1$, and they form a set of vertex-disjoint paths in G.

Call a bi-directional edge with colors $i-1, i+1$ a *cyclic edge*. We can form a directed acyclic graph D_i by *grouping* each maximal path in $\mathcal{T}_{i-1}^{-1} \cup \mathcal{T}_{i+1}^{-1} \cup \mathcal{T}_i$ with cyclic bi-colored edges (call such a path a *cyclic maximal path*) into a single vertex. Here the maximal paths P_i with cyclic bi-colored edges are the vertices of D_i, and for two such paths P_i and P_j, there is a directed edge from P_i to P_j in D_i whenever there is a directed (not cyclic) edge (u, v) in $\mathcal{T}_{i-1}^{-1} \cup \mathcal{T}_{i+1}^{-1} \cup \mathcal{T}_i$ for some $u \in P_i$ and $v \in P_j$. Badent et al. [2] show that D_i is acyclic and they suggest to obtain an ordered path partition by taking a topological order of the vertices D_i and for each vertex u of G, assigning k as its label where $u \in U$ for some cyclic maximal path U in D_i and k is the rank of U in the topological ordering of D_i. However, the resulting ordered path partition is not necessarily compatible with $(\mathcal{T}_1, \mathcal{T}_2, \mathcal{T}_3)$ and Fig. 11 shows an example. Instead, before grouping the cyclic maximal paths, we augment the graph $\mathcal{T}_{i-1}^{-1} \cup \mathcal{T}_{i+1}^{-1} \cup \mathcal{T}_i$ by adding some additional directed edges. We prove that the augmented graph is acyclic and the partial order defined by it is consistent with the partial order defined by D_i (we call this the *partial order defined by* $\mathcal{T}_{i-1}^{-1} \cup \mathcal{T}_{i+1}^{-1} \cup \mathcal{T}_i$). An ordered path partition Π for G is *consistent* with the partial order defined by D_i, $i \in \{1, 2, 3\}$, if for any two vertices u, v of G such that $u \in U$, $v \in V$ for some cyclic maximal paths U, V, if there is a directed path from U to V in D_i, then the label of u is smaller than that of v in Π. A topological order of the augmented graph (after grouping all cyclic maximal paths) induces a compatible ordered path partition.

Lemma 1. *Let $(\mathcal{T}_1, \mathcal{T}_2, \mathcal{T}_3)$ be a Schnyder wood of a 3-connected plane graph G with three specified vertices v_1, v_2, v_3 in that counterclockwise order on the outer face. Then for $i \in \{1, 2, 3\}$, one can compute in linear time an ordered path partition Π_i compatible with $(\mathcal{T}_1, \mathcal{T}_2, \mathcal{T}_3)$ such that Π_i has (v_{i-1}, v_{i+1}) as the base-pair and v_i as the head. The ordered path partition Π_i is consistent with the partial order defined by $\mathcal{T}_{i-1}^{-1} \cup \mathcal{T}_{i+1}^{-1} \cup \mathcal{T}_i$.*

Proof. Consider the directed acyclic graph D_i created by grouping each cyclic maximal path of $\mathcal{T}_{i-1}^{-1} \cup \mathcal{T}_{i+1}^{-1} \cup \mathcal{T}_i$ into a single vertex. By [11], G contains no directed cycle in $\mathcal{T}_{i-1}^{-1} \cup \mathcal{T}_{i+1}^{-1} \cup \mathcal{T}_i$. Hence D_i is acyclic. Each vertex in D_i has at least two predecessors, one in $\mathcal{T}_{i-1}^{-1}$ and one in $\mathcal{T}_{i+1}^{-1}$. Therefore one can compute an ordered path partition of G as follows. We compute a topological ordering of D_i. Then for each vertex u of G,

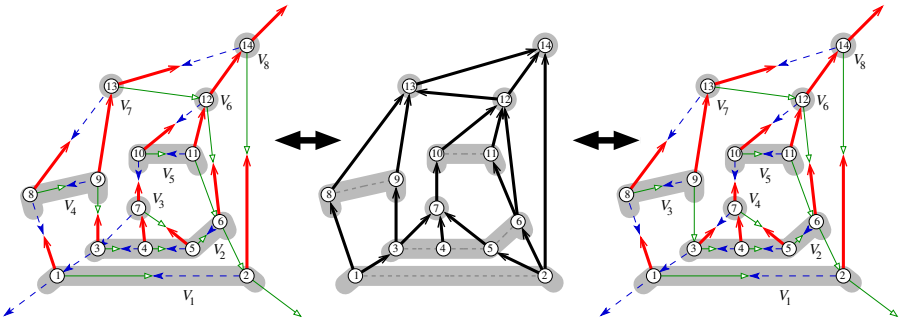

Fig. 11: Two ordered path partitions with their compatible Schnyder woods (left and right) that gives the same acyclic graph D_i after reversing the direction of the edges in two trees and grouping all cyclic maximal paths. Thus starting with either Schnyder wood can give either ordered path partition by the algorithm in [2].

we assign label k to u, where $u \in U$ for some cyclic maximal path U (i.e., a vertex of D_i) and k is the rank of U in the topological ordering; see [2] for details. However, the ordered path partition obtained by this procedure might not be compatible with $(\mathcal{T}_1, \mathcal{T}_2, \mathcal{T}_3)$; in particular for a vertex u of G, its parent in $\mathcal{T}_i$ might not be its highest-labeled successor; see Fig. 11.

In order to ensure compatibility between the Schnyder wood and the obtained ordered path partition, we augment $\mathcal{T}_{i-1}^{-1} \cup \mathcal{T}_{i+1}^{-1} \cup \mathcal{T}_i$ by adding some extra edges, before grouping the cyclic maximal paths. In particular, for each vertex v of G, let r be its parent in $\mathcal{T}_i$, g_1, ..., g_p its children in $\mathcal{T}_{i-1}$ in the clockwise order around u, and b_1, ..., b_q its children in $\mathcal{T}_{i+1}$ in the counterclockwise order around u; see Fig. 12(a). Thus, the vertices $L = g_1, \ldots, g_p, r, b_q, \ldots, b_1$ appear consecutively around u in that clockwise order. For each vertex u, we add edges from g_j, $j \in \{1, \ldots, p\}$ to the next vertex in L (i.e., g_{j+1} when $j < p$, and r when $j = p$). Similarly, we add edges from b_j, $j \in \{1, \ldots, q\}$ to the previous vertex in L (i.e., b_{j+1} when $j < q$, and r when $j = q$). After the addition of the extra edges, we group each cyclic maximal path into a single vertex. Call the augmented directed graph (after grouping the cyclic maximal paths) H_i. Note that H_i can equivalently be seen as an augmentation of D_i as follows. For each additional edge $e = (x, y)$ inserted in $\mathcal{T}_{i-1}^{-1} \cup \mathcal{T}_{i+1}^{-1} \cup \mathcal{T}_i$, we can think of inserting an edge $e' = (U, V)$, where U, V are two cyclic maximal paths of $\mathcal{T}_{i-1}^{-1} \cup \mathcal{T}_{i+1}^{-1} \cup \mathcal{T}_i$ grouped into vertices in D_i, and $u \in U$, $v \in V$. We now prove that the directed graph H_i is acyclic. We prove this for H_3 as the arguments for H_1, H_2 are analogous. Before we proceed we need the concept of a *plane st-digraph*.

A directed acyclic plane graph S is a *plane st-digraph* (or *plane bipolar graph*) [24, 26] if it has a *source* s and a *sink* t on the outer face such that all edges incident to s are outgoing, all edges incident to t are incoming and any vertex u of S other than s and t, is incident to at least one incoming and at least one outgoing edge. Each face f in a plane st-digraph S has a local source s_f and a local sink t_f, such that the boundary of f is split into two directed paths from s_f to t_f. Call these two directed paths *left* and

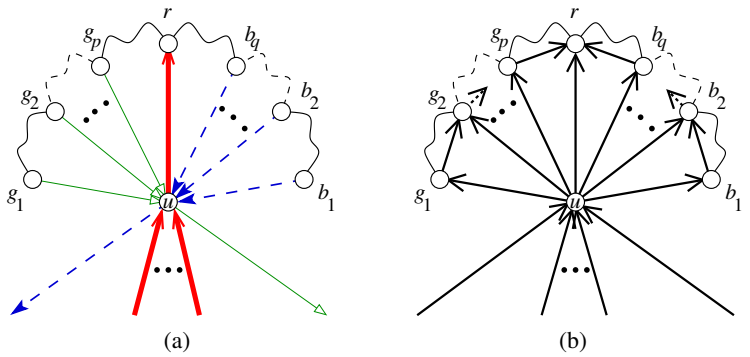

Fig. 12: (a) Coloring and orientation of the edges around a vertex u of the graph G in a Schnyder wood $(\mathcal{T}_1, \mathcal{T}_2, \mathcal{T}_3)$. (b) Orientation of the edges in $\mathcal{T}_2^{-1} \cup \mathcal{T}_1^{-1} \cup \mathcal{T}_3$ together with the extra edges added for the vertex u of G.

right, so that the left path comes before right path in the clockwise order around s_f. The following observation trivially follows from [26].

Observation 1. *Let S be a plane st-digraph with a face f, and let x and y be two non-adjacent vertices on f. Then S remains a plane st-digraph after adding the edge (x, y), if one of the following conditions holds:*

(i) x, y are either both on the left path of f, or both on the right path of f, where x comes before y on either path,

(ii) one of x, y is on the left path of f, the other on the right path of f, $x \neq t_f$, $y \neq s_f$.

Consider the graph D_3. Recall that D_3 is the graph obtained by grouping each cyclic maximal path of $\mathcal{T}_2^{-1} \cup \mathcal{T}_1^{-1} \cup \mathcal{T}_3$ into a vertex. By Lemma 6, D_3 is acyclic. Furthermore each vertex u, other than v_1, v_2 (which are grouped together) and v_3, has at least one incoming edge (from the parent of u in $\mathcal{T}_1$ or $\mathcal{T}_2$) and at least one outgoing edge (to the parent of u in $\mathcal{T}_3$). Thus D_3 is a plane st-digraph with source v_1 (which is grouped with v_2) and sink v_3. We prove that with the addition of the extra edges, the graph H_3 remains a plane st-digraph. To see this, we view the addition of each extra edge $e = (x, y)$ as occurring both in $\mathcal{T}_2^{-1} \cup \mathcal{T}_1^{-1} \cup \mathcal{T}_3$, and accordingly in H_3 (i.e., between the groups that x, y belong to). Consider an arbitrary vertex u of G, and define $L = g_1, \ldots, g_p, r, b_q, \ldots, b_1$ as before, where r is its parent in $\mathcal{T}_3$, $g_1, \ldots, g_p$ its children in $\mathcal{T}_2$ in the clockwise order, and $b_1, \ldots, b_q$ its children in $\mathcal{T}_1$ in the counterclockwise order; see Fig. 12(a). Consider the orientation of the edges between u and the vertices in L; see Fig. 12(b). Each consecutive vertex pair in L shares a common face with u, where u is the local source. We therefore first investigate the orientation of the edges around a face of G, in $\mathcal{T}_2^{-1} \cup \mathcal{T}_1^{-1} \cup \mathcal{T}_3$.

Consider an arbitrary face f of G. An edge (or half-edge) is *clockwise* if its orientation is clockwise with respect to the inside of f; otherwise it is *counterclockwise*. Again an edge (or half-edge) in color $i \in \{1, 2, 3\}$ if it belongs to the Schnyder tree $\mathcal{T}_i$. Then by [11], the edges on the boundary of f can be partitioned into at most six consecutive sets in the clockwise order around f as shown in Fig. 13(a):

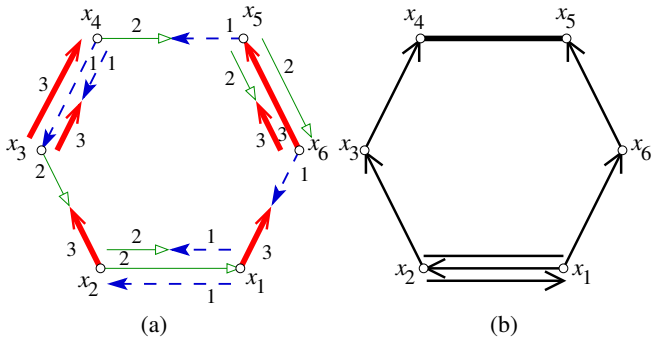

Fig. 13: (a) Coloring and orientation of the edges around a face f of G in a Schnyder wood $(\mathcal{T}_1, \mathcal{T}_2, \mathcal{T}_3)$. (b) Orientation of the edges of f in $\mathcal{T}_2^{-1} \cup \mathcal{T}_1^{-1} \cup \mathcal{T}_3$. The cyclic edges are shown as undirected.

(i) one edge from the set {clockwise in color 1, counterclockwise in color 2, bi-colored with a clockwise 1 and counterclockwise 2}
(ii) zero or more edges bi-colored in counterclockwise 2 and clockwise 3
(iii) one edge from the set {clockwise in color 3, counterclockwise in color 1, bi-colored with a clockwise 2 and counterclockwise 1}
(iv) zero or more edges bi-colored in counterclockwise 1 and clockwise 2
(v) one edge from the set {clockwise in color 2, counterclockwise in color 3, bi-colored with a clockwise 2 and counterclockwise 3}
(vi) zero or more edges bi-colored in counterclockwise 3 and clockwise 1

Fig. 13(b) shows the direction of the edges of f in $\mathcal{T}_2^{-1} \cup \mathcal{T}_1^{-1} \cup \mathcal{T}_3$ (note that some of the edges are drawn undirected since they form cyclic paths in $\mathcal{T}_2^{-1} \cup \mathcal{T}_1^{-1} \cup \mathcal{T}_3$ and hence will be grouped in D_3).

Now consider some child g_j of u in $\mathcal{T}_2$. We distinguish two cases.

Case 1, $j < p$**.** In this case, in the face f_j of G containing g_j, g_{j+1} and u, the two edges incident on u are counterclockwise in color 2 and clockwise in color 2, respectively. Looking at the face in Fig. 13(a), this can only occur when (i) x_1 and x_6 are the same vertex, which is identified with u, and (ii) x_2, x_5 are identified with g_j, g_{j+1}, respectively. Thus, the path between g_j, g_{j+1} on f_j is directed in D_3, and hence is part of the left path of f_j (here g_{j+1} is the sink of f_j). Thus by Observation 1, graph H_3 remains a plane st-digraph after adding the edge (g_j, g_{j+1}).

Case 2, $j = p$**.** In this case, in the face f_p of G containing g_p, r and u, the two edges incident on u are counterclockwise in color 2 and counterclockwise in color 3, respectively. This can only occur when (i) x_1, x_6 are the same vertex, which is identified with u, and x_2, x_5 are identified with g_p, r, respectively, or when (ii) x_1, x_2, x_6 are identified with u, g_p, r, respectively. In the former case, the argument from the previous paragraph shows that adding the edge (g_p, r) preserves the acyclicity of H_3. In the latter case, the source of f_p is $u = x_1 \neq x_6 = r$, the sink of f_p is $x_5 \neq x_2 = g_p$, $g_p = x_2$ is on the left path and $r = x_6$ is on the right path of f_p. Thus by Observation 1, graph H_3 remains a plane st-digraph after adding the edge (g_p, r).

Similarly adding the edges (b_j, b_{j+1}), $j < q$ and edge (b_q, r) preserves the acyclicity of H_3. In particular for $j < q$, similar arguments to those in **Case 1** apply, and by Observation 1, the graph H_3 remains a plane st-digraph. On the other hand, for $j = q$, arguments similar to those in **Case 2** shows that H_3 remains a plane st-digraph. Thus with the addition of all these edges H_3 is plane st-digraph and hence acyclic. H_1 and H_2 can be shown to be acyclic with analogous arguments.

Thus for $i \in \{1, 2, 3\}$, we can compute an ordered path partition consistent with the partial order defined by $\mathcal{T}_{i-1}^{-1} \cup \mathcal{T}_{i+1}^{-1} \cup \mathcal{T}_i$ as follows. We compute a topological ordering of H_i. Then for each vertex u of G, we assign label k to u, where $u \in U$ for some cyclic maximal path U (i.e., a vertex of H_i) and k is the rank of U in the topological ordering of H_i. This ordered path partition is compatible with $(\mathcal{T}_1, \mathcal{T}_2, \mathcal{T}_3)$ since for each vertex u, the parents of u in $\mathcal{T}_{i-1}$ and in $\mathcal{T}_{i+1}$ are the leftmost and rightmost predecessors (due to the embedding) and the parent r in $\mathcal{T}_i$ is the highest-labeled successor (since from all other successors of u, there is a directed path to r containing the added edges).

The time complexity of this algorithm is linear. Computing the directed graph D_i, $i \in \{1, 2, 3\}$ can be done in linear time, as in [2]. Addition of the extra edges takes $\sum_{v \in V(G)} deg(v) = 2|E(G)| = \mathcal{O}(n)$ time. Finally the topological ordering of H_i can be computed in linear time. □

Fig. 14 illustrates the three ordered path partitions computed from a Schnyder wood of a 3-connected plane graph using the algorithm described above.

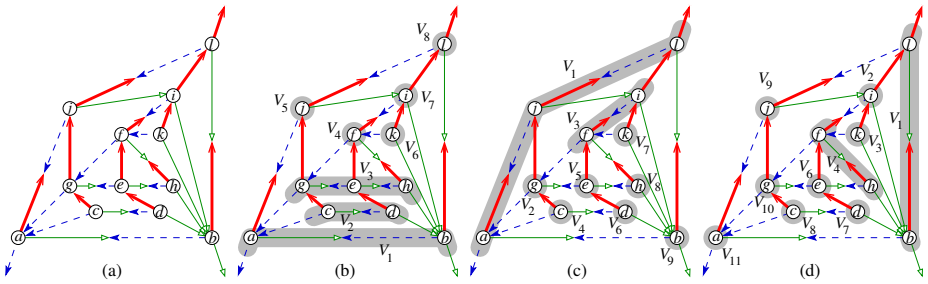

Fig. 14: (a) A Schnyder wood $(\mathcal{T}_1, \mathcal{T}_2, \mathcal{T}_3)$ in a 3-connected plane graph G, (b)–(d) the three compatible ordered path partitions computed from $(\mathcal{T}_1, \mathcal{T}_2, \mathcal{T}_3)$ using the algorithm described in the proof of Lemma 1.

B.3 Orthogonal Surfaces

Here we review the notion of orthogonal surfaces, which we use in the proof for Theorem 1; see [11] for more details. A point p in $\mathbb{R}^3$ *dominates* another point q if the coordinate of p is greater than or equal to q in each dimension; p and q are *incomparable* if neither of p nor q dominates the other. Given a set M of incomparable points, an *orthogonal surface* defined by M is the geometric boundary of the set of points that dominate at least one point of M. For two points p and q, their *join*, $p \vee q$ is obtained by taking the maximum coordinate of p, q in each dimension separately. The *minimums*

(*maximums*) of an orthogonal surface S are the points of S that dominate (are dominated by) no other point of S. An orthogonal surface S is *rigid* if for each pair of points p and q of M such that $p \vee q$ is on S, $p \vee q$ does not dominate any point other than p and q. An orthogonal surface is *axial* if it has exactly three unbounded orthogonal arcs. Rigid axial orthogonal surfaces are known to be in one-to-one correspondence with Schnyder woods of 3-connected plane graphs [11] and the rigid axial orthogonal surfaces S and S^* corresponding to a Schnyder wood and its dual coincide with each other, where the maximums of S are the minimums of S^* and vice versa.

B.4 Algorithm for Primal-Dual Representation

Here we prove Theorem 1. Specifically, we describe a linear-time algorithm that computes a box-contact representation for the primal graph and the dual graph separately and then fits them together to obtain the desired result. We compute the coordinates of the boxes based on a Schnyder wood. This guarantees that the boundary for the primal (dual) representation induces an *orthogonal surface* compatible with the dual (primal) Schnyder wood. Since the orthogonal surfaces for a Schnyder wood and its dual coincide topologically, we can fit together the primal and the dual box-contact representation to obtain a desired representation. Note that some of the concepts and proof techniques in this section mirrors the ones in [5], although they are generalized to 3-connected graphs.

To avoid confusion, we denote a connected region in a plane embedding of a graph by a *face*, and a side of a 3D shape by a *facet*. For a 3D box R, call the facet with highest (lowest) x-coordinate as the x^+-facet (x^--facet) of R. The y^+-facet, y^--facet, z^+-facet and z^--facets of R are defined similarly. For convenience, we sometimes denote the x^+-, x^--, y^+-, y^--, z^+- and z^--facets of R as the *right*, *left*, *front*, *back*, *top* and *bottom* facets of R, respectively.

Theorem 1. *Every 3-connected plane graph $G = (V, E)$ admits a proper primal-dual box-contact representation in 3D and it can be computed in $\mathcal{O}(|V|)$ time.*

Proof. We compute a box-contact representation for the primal graph and the dual graph separately and then fits them together to obtain the desired result. Let v_1, v_2 and v_3 be three vertices on the outer face of G in the counterclockwise order. We compute a Schnyder wood $(\mathcal{T}_1, \mathcal{T}_2, \mathcal{T}_3)$ such that for $i \in \{1, 2, 3\}$, $\mathcal{T}_i$ is rooted at v_i. We then compute three ordered path partition compatible with $(\mathcal{T}_1, \mathcal{T}_2, \mathcal{T}_3)$ using the result in Lemma 1, and use these three ordered path partition to compute the coordinates of the 3D boxes, that form a contact representation Γ. We compute the dual representation Γ' in the same way, using the dual Schnyder wood of $(\mathcal{T}_1, \mathcal{T}_2, \mathcal{T}_3)$. We then show that these two representation induce the same orthogonal surface and hence can fit together to form a primal-dual proper box-contact representation.

Note that computation of the box-contact representation from a Schnyder wood mirrors the ideas in [5]. However we need to generalize the the ideas for 3-connected planar graphs, for which showing the correspondance between ordered path partitions and Schnyder woods is non-trivial. Furthermore, we need to exploit the relation between an orthogonal surface with a primal and a dual Schnyder wood to argue that the two representations fit together.

We now describe the algorithm to compute the primal representation Γ from a Schnyder wood $(\mathcal{T}_1, \mathcal{T}_2, \mathcal{T}_3)$. As we already mentioned the computation for dual representation is analogous. By Lemma 1, for $i \in \{1, 2, 3\}$, one can compute a compatible ordered path partition with the base-pair (v_{i-1}, v_{i+1}) and head v_i, which is consistent with the partial order defined by $\mathcal{T}_{i-1}^{-1} \cup \mathcal{T}_{i+1}^{-1} \cup \mathcal{T}_i$. Denote by $<_X$, $<_Y$ and $<_Z$ the three ordered path partitions compatible with $(\mathcal{T}_1, \mathcal{T}_2, \mathcal{T}_3)$, that are consistent with $\mathcal{T}_3^{-1} \cup \mathcal{T}_2^{-1} \cup \mathcal{T}_1$, $\mathcal{T}_1^{-1} \cup \mathcal{T}_3^{-1} \cup \mathcal{T}_2$, and $\mathcal{T}_2^{-1} \cup \mathcal{T}_1^{-1} \cup \mathcal{T}_3$, respectively. We use these three ordered path partitions to define our box-contact representation for G.

For a vertex u, let $x_M(u)$, $y_M(u)$, and $z_M(u)$ be the labels of u in the ordered path partitions $<_X$, $<_Y$, and $<_Z$, respectively. Define $x_m(u) = x_M(b)$, $y_m(u) = y_M(g)$ and $z_m(u) = z_M(r)$, where b, g and r are the parents of u in $\mathcal{T}_1$, $\mathcal{T}_2$ and $\mathcal{T}_3$, respectively, whenever these parents are defined. For each of the three special vertices v_i, $i \in \{1, 2, 3\}$, the parent is not defined in $\mathcal{T}_i$. We assign $x_m(v_1) = 0$, $y_m(v_2) = 0$ and $z_m(v_3) = 0$.

Now for each vertex u of G, let the the region $[x_M(u), x_m(u)] \times [y_M(u), y_m(u)] \times [z_M(u), z_m(u)]$ be the box $R(u)$ representing u. Denote by R the set of all boxes $R(u)$ for the vertices u of G. We show in Lemma 7 that R yields a box-contact representation for G. Furthermore, for each edge (u, v) of G, if (u, v) is uni-colored then $R(u)$ and $R(v)$ make a proper contact. Otherwise, assume w.l.o.g. that (u, v) is bi-colored with colors 1 (oriented from u to v) and 2 (oriented from v to u). Then $x_m(u) = x_M(v)$, $y_M(u) = y_m(v)$, $z_M(u) = z_M(v)$; $R(u)$ and $R(v)$ make a non-proper contact along the line-segment $\{x_m(u)\} \times \{y_m(v)\} \times [z_M(u), z^*]$, where $z^* = \min\{z_m(u), z_m(v)\}$. However since v is the only parent of u in $\mathcal{T}_1$ and u is the only parent of v in $\mathcal{T}_2$, by Lemma 7, the x^+-facet of $R(u)$ and the y^+-facet of $R(v)$ do not make a proper contact with any box. Hence either extending $R(u)$ in the positive x-direction or extending $R(v)$ in positive y-direction by $\epsilon = 0.5$ makes the contact between $R(u)$ and $R(v)$ proper without creating any overlap or unnecessary contacts between the boxes. We thus obtain a proper box-contact representation Γ for the primal graph G.

In order to see how we fit the primal and the dual representation together, consider the orthogonal surface induced by Γ. Each vertex v of G corresponds to the $x^-y^-z^-$-corner p of $R(v)$. The three outgoing edges of v in the Schnyder wood can be drawn on the surface from p in the directions x^+, y^+, z^+; see Fig. 4. Thus the topology of this (rigid axial) orthogonal surface corresponds to the one uniquely defined for both the Schnyder wood and its dual in [11]. Since the primal and the dual Schnyder wood corresponds to the same (rigid axial) orthogonal surface, the boundary of Γ' (after possible scaling) exactly matches $B - \Gamma$, where B is the bounding box of Γ. Finally we replace the three boxes for the three outer vertices of G with a single shell-box, which forms the boundary of the entire representation.

It is easy to see that the above algorithm runs in $\mathcal{O}(|V|)$ time. A Schnyder wood for G and the dual Schnyder wood for the dual of G can be computed in linear time [11]. For both the primal graph and the dual graph, the three ordered path partitions can then be computed in linear time from these Schnyder woods, due to Lemma 1. The coordinates of the boxes are then directly assigned in constant time per vertex. Finally the primal and the dual representation can be combined together by reflecting (and possibly scaling) the dual representation, which can also be done in linear time. □

Lemma 7 shows the correctness for the construction in the proof of Theorem 1; specifically, it shows that the boxes computed in the construction induce a contact representation for G.

Lemma 7. *The set of all boxes $R(u)$ for the vertices u of G induces a contact representation of G, where for each vertex u, the x^+-, y^+-, z^+-facets of $R(u)$ touch the boxes for the parents of u in $\mathcal{T}_1$, $\mathcal{T}_2$, $\mathcal{T}_3$, respectively, and the x^--, y^--, z^--facets of $R(u)$ touch the boxes for the children of u in $\mathcal{T}_1$, $\mathcal{T}_2$, $\mathcal{T}_3$, respectively. Furthermore for each edge (u, v) of G, the contact between $R(u)$ and $R(v)$ is proper if and only if (u, v) is uni-colored.*

Proof. We prove the lemma by showing the following two claims: (i) for each edge (u, v) of G, the two boxes $R(u)$ and $R(v)$ make contact in the specified facets, (ii) for any two vertices u and v of G, the two boxes $R(u)$ and $R(v)$ are interior-disjoint.

(i) Take an edge (u, v) of G. If (u, v) is uni-colored in G, assume w.l.o.g. that it has color 3 and is directed from u to v. By construction, $z_m(u) = z_M(v)$. We now show that $x_M(v) < x_M(u) < x_m(v)$ and $y_M(v) < y_M(u) < y_m(v)$, which implies the correct contact between $B(u)$ and $B(v)$. Since (u, v) is in $\mathcal{T}_3$ and the ordered path partitions $<_X$ and $<_Y$ are consistent with $\mathcal{T}_3^{-1}$, $x_M(v) < x_M(u)$ and $y_M(v) < y_M(u)$. To show that $x_M(u) < x_m(v)$, consider the parent b of v in $\mathcal{T}_1$. Then $x_m(v) = x_M(b)$. Furthermore, before computing the topological order to find $<_X$, we added the directed edge (u, b); thus $x_M(u) < x_M(b) = x_m(v)$. The proof that $y_M(u) < y_m(v)$ is symmetric.
If (u, v) is bi-colored with colors, w.l.o.g., 1 (orientated from u to v) and 2 (from v to u), then by construction $x_m(u) = x_M(v)$ and $y_M(u) = y_m(v)$. (u, v) is bi-colored in 1, 2, so $z_M(u) = z_M(v)$. Thus, $R(u)$, $R(v)$ make non-proper contact in the correct facets.

(ii) Now we show that for any two vertices u and v of G, $R(u)$ and $R(v)$ are interior-disjoint. By the properties of Schnyder woods, from any vertex u of G, there are three vertex-disjoint paths $P_1(u)$, $P_2(u)$, $P_3(u)$ where $P_i(u)$ is a directed path from u to v_i of edges colored i, $i \in \{1, 2, 3\}$. We first claim that for some $i, j \in \{1, 2, 3\}$, $i \neq j$, there is a directed path from u to v, or from v to u in $\mathcal{T}_i \cup \mathcal{T}_j^{-1}$. The claim holds trivially if u is on the directed path $P_i(v)$, or v is on the directed path $P_i(u)$, for some $i \in \{1, 2, 3\}$. Otherwise, assume that v is in the region between $P_2(u)$, and $P_3(u)$. Then the path $P_1(v)$ intersects either $P_2(u)$, and $P_3(u)$ at some vertex w. Assume w.l.o.g. that w is on $P_2(u)$. Then the path P that follows $P_1(v)$ from v to w, and then follows $P_2^{-1}(u)$ from w to u is directed in $\mathcal{T}_2^{-1} \cup \mathcal{T}_1$ (here $P_2^{-1}(u)$ is the path $P_2(u)$ with all the directions reversed). Hence, assume that there is a path from u to v in $\mathcal{T}_1 \cup \mathcal{T}_2^{-1}$. By definition, $x_m(u) \leq x_M(v)$ and thus $R(u)$ and $R(v)$ are interior-disjoint.

□

The construction for a primal-dual box-contact representation of a 3-connected plane graph G in Theorem 1 has another interpretation. Start with the orthogonal surface S corresponding to both a Schnyder wood of G and its dual. This orthogonal surface S creates two half-spaces on either side of S: extend boxes from S in these half-spaces, so that (i) the boxes are interior-disjoint and (ii) they induce box-contact representations

for the primal and dual graphs. However, how to extend the corners and why such a construction yields a proper box-contact representation seems to require the same kinds of arguments that we provided in this section. A "proof from the book" for Theorem 1, using topological properties of the orthogonal surface, is a nice open problem.

C Additional Figures

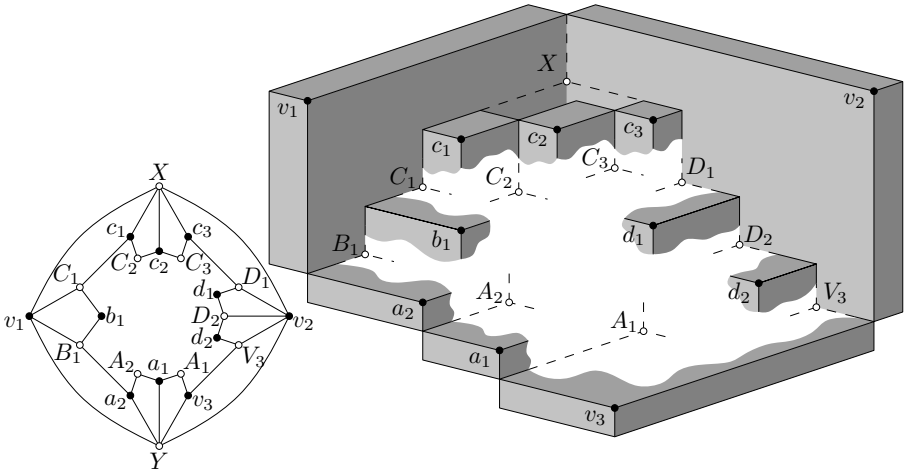

Fig. 15: Part of an optimal 1-planar graph and its partial proper box contact representation

Additional References

22. D. Avis and M. E. Houle. Computational aspects of Helly's theorem and its relatives. *International Journal of Computational Geometry and Applications*, 5(4):357–367, 1995.
23. N. Bonichon, S. Felsner, and M. Mosbah. Convex drawings of 3-connected plane graphs. *Algorithmica*, 47(4):399–420, 2007.
24. H. de Fraysseix and P. O. de Mendez. On topological aspects of orientations. *Discrete Mathematics*, 229(1–3):57–72, 2001.
25. H. de Fraysseix, J. Pach, and R. Pollack. How to draw a planar graph on a grid. *Combinatorica*, 10(1):41–51, 1990.
26. G. Di Battista, P. Eades, R. Tamassia, and I. G. Tollis. *Graph Drawing: Algorithms for the Visualization of Graphs*. Prentice Hall, Englewood Cliffs, NJ, 1999.
27. G. Kant. Drawing planar graphs using canonical ordering. *Algorithmica*, 16(1):4–32, 1996.
28. W. Schnyder. Embedding planar graphs on the grid. In D. S. Johnson, editor, *SODA*, pages 138–148. SIAM, 1990.